JPL D-102349

Multiangle SpectroPolarimetric Imager

GroundMSPI Data Quality Statement: ACEPOL Campaign

Christine L. Bradley, Abigail M. Nastan, Gerard van Harten, David J. Diner (PI), Michael J. Garay, Brian E. Rheingans, Carol J. Bruegge, Veljko M. Jovanovic, Michael A. Bull, Irina N. Tkatcheva, Feng Xu
Corresponding author: Abigail.m.nastan@jpl.nasa.gov

Campaign	
Name	ACEPOL (Aerosol Characterization from Polarimeter and Lidar)
Dates	October 25 and November 7, 2017
Locations	Rosamond Dry Lake and Fresno, California
Airborne instruments	AirMSPI, AirHARP, CPL, HSRL-2, RSP, SPEX
Ground-based remote sensing instruments	GroundMSPI, FieldSpecPro by Analytical Spectral Devices, Microtops II sunphotometer by Solar Light, Reagan sunphotometer

GroundMSPI Overview of Data Calibration and Processing to Level 1B2	
Data DOI	10.5067/GROUND/GROUNDMSPI/ACEPOL/RADIANCE_v009
Data Delivery Version	V009
PGE Software Version	8.4
Lab. Cal. Software Version	6.5 (5.0 for lincal)
Radiometric Calibration	25 February 2016
Polarimetric Calibration	23 February 2016
Lin. Cal. File	gndmspi_lincal_20130523_v5.0.dat
Pol. Cal. File	gndmspi_polcal_20160223_v6.5.dat
Rad. Calibration File	gndmspi_radcal_20160225_v6.5.dat

Jet Propulsion Laboratory
California Institute of Technology

1 October 2018

JPL D-102349

Ground-Based Multiangle SpectroPolarimetric Imager (GroundMSPI)

GroundMSPI Data Quality Statement: ACEPOL Campaign

APPROVALS:

David J. Diner

AirMSPI Principal Investigator

Approval signatures are on file with the AirMSPI Project.
To determine the latest released version of this document, consult the AirMSPI website (http://airbornescience.jpl.nasa.gov/instruments/airmspi/).

Jet Propulsion Laboratory
California Institute of Technology

Document Change Log

Revision	Date	Affected Portions and Description
	1 September 2018	Original release

Which Product Versions Does this Document Cover?

Product Filename Prefix	Version Number in Filename	Brief Description
GroundMSPI_L1B2	V009	L1B2 Rectified and Co-Registered Radiance and Polarization Data

TABLE OF CONTENTS

1 INTRODUCTION

The purpose of this document is to describe the data quality of the GroundMSPI L1B2 products specifically in support of the Aerosol Characterization from Polarimeter and Lidar (ACEPOL) flight and field campaign, which was based out of NASA Armstrong Flight Research Center (AFRC) in Palmdale, CA. GroundMSPI imagery was acquired on 25 October and 7 November 2017, when the GroundMSPI instrument was situated at Rosamond Dry Lake and Fresno, CA, respectively.

1.1 GroundMSPI L1B2 Products

The Ground-based Multiangle SpectroPolarimetric Imager (GroundMSPI) Level 1B2 products contain radiometric and polarimetric observations of clouds, aerosols, and the surface of the Earth made from a ground-based vantage point. The GroundMSPI instrument is mounted in a two-axis gimbaled mount to accurately point in azimuth and elevation and acquires data using a sweep mode. GroundMSPI has a ±15° horizontal field of view across a 1536-pixel-wide detector, for a spatial resolution of 1.2 arcmin. For example, for a target 100 m away, the GroundMSPI spatial resolution is 3 cm and the scene width is about 50 m. Files are distributed in HDF-EOS-5 format.

The instrument reports for eight spectral bands (355, 380, 445, 470, 555, 660, 865, and 935 nm) the incident radiance (Stokes *I)*, complemented with the linear polarization state (Stokes *Q* and *U*) in three of the bands (470, 660, and 865 nm) for a total of 14 channels.

1.2 GroundMSPI Data Processing and Distribution

The MISR Science Computing Facility (SCF) at the Jet Propulsion Laboratory (JPL) supports the development of GroundMSPI science algorithms and software, instrument calibration and performance assessment, and also provides quality assessment and data validation services with respect to GroundMSPI Science Data Processing (SDP). The MISR SCF is used to perform the standard processing of the GroundMSPI data. After GroundMSPI data processing is complete, the standard output products are archived and made available to users via the Langley Research Center (LaRC) Atmospheric Science Data Center (ASDC) client services. See https://eosweb.larc.nasa.gov/project/airmspi/airmspi_table.

1.3 Controlling Documents

1) Multiangle Spectropolarimetric Imager (MSPI) Algorithm Theoretical Basis Document Rev. B Draft, November 2009 (or latest version).

1.4 Related Documents

1) Data Product Specification for the GroundMSPI Level 1B2 Products (V009), JPL D-102348, September 2018 (or latest version).

2 RADIOMETRIC CALIBRATION

2.1 Laboratory Calibration

Laboratory radiometric calibration of the GroundMSPI instrument (Diner et al., 2012) was conducted on 25 February 2016 by observing the output port of a 1.65 m integrating sphere. The sphere illuminates the entire field of view of the instrument. Data were collected at multiple light levels and the sphere output was monitored with an Analytical Spectral Devices (ASD) FieldSpec Pro spectrometer in order to generate a digital number (DN) vs. radiance regression for each pixel. The GroundMSPI line arrays have 1536 pixels in each channel. Offset levels are determined from observations in 100 pixels at the end of each array that are shielded from illumination; hence only 1436 pixels in each line collect image data. After correction for non-linearity (lincal), gain factors are computed on a per-pixel basis for each channel. The 14 spectral channels of the instrument measure incident radiance at wavelengths close to 355, 380, 445, 470, 555, 660, 865, and 935 nm (8 bands). In keeping with Stokes parameter nomenclature, the polarization channels report I, Q, and U, where I is the total measured radiance. The Stokes parameters Q (excess of horizontally over vertically polarized light) and U (excess of 45° over 135° polarized light) are reported for the bands at 470, 660, and 865 nm. Note that the GroundMSPI instrument does not have a separate radiance-only channel at 470 nm. The radiance reported in the GroundMSPI data products for this channel is obtained independently from the demodulated 470Q and 470U channel data and is the mean of the values derived from these two channels.

Although gain factors are derived on a per-pixel basis, residual striping can appear in images, particularly in the UV bands. It is believed that this striping is the result of out-of-band spectral leakage due to physical imperfections in the focal plane filter.

2.2 Calibration Traceability

GroundMSPI calibrations are traceable to *Système international* (SI) Units, via National Institute of Standards and Technology (NIST) standards. For laboratory calibrations, this is accomplished through a reference 20.32 cm (8 inch) integrating sphere, calibrated annually by the vendor, Gooch & Housego (http://goochandhousego.com/).

3 SPECTRAL CALIBRATION

The spectral response function (SRF) of GroundMSPI is assumed similar to AirMSPI (Diner et al., 2013a) given they employ similar focal plane array and filters. GroundMSPI uses the AirMSPI SRF for spectral calibration. Determination of the detailed SRF of each AirMSPI channel has been made based on the laboratory calibration of 9 December 2013. A monochromator was used for this purpose. The SRF is equal to the camera response to monochromatic light normalized by a silicon diode response. The monochromator provided wavelength scans from 300 to 2500 nm. Two sources were used in separate spectral scans of all channels — a Luxim Light Emitting Plasma lamp for ultraviolet-blue, and a quartz-halogen lamp for the remaining visible and near-infrared channels. The results of the AirMSPI calibration are shown in Table 1 and Figure 2.

In the current GroundMSPI product release (V009), center wavelengths, effective (equivalent square-band) bandwidths, and effective (equivalent square-band) transmittances are calculated by applying the moments method of Palmer (1984) to the AirMSPI normalized spectral response of each band over the range 300-1100 nm. Solar irradiances are weighted by the total-band spectral response. The Wehrli (1985) extraterrestrial solar spectrum was used for this purpose. These values are provided in Table 1 below, and represent the total-band response.

In general, radiometric response at wavelengths far from the "in-band" spectral region is estimated at $< 10^{-4}$ of the peak response, though as noted above, a larger amount of out-of-band leakage is present in a small subset of pixels in the UV bands, leading to striping in a portion of the UV images.

Table 1 – Total-band effective center wavelength, bandwidth and transmittance, and total-band weighted solar irradiance E_0 [W m^{-2} nm^{-1}] at 1 AU

Channel Name	Center Wavelength (nm)	Effective Bandwidth (nm)	Effective Transmittance	Solar Irradiance (W m^{-2} nm^{-1})
355I	355.1	47.7	0.609	1.002
380I	377.2	40.4	0.750	1.079
445I	443.3	46.0	0.799	1.861
470I	469.1	45.5	0.824	2.000
470Q	469.4	45.0	0.837	1.999
470U	468.8	46.0	0.815	2.000
555I	553.5	38.6	0.758	1.857
660I	659.2	45.2	0.835	1.555
660Q	659.1	43.8	0.881	1.556
660U	659.1	48.2	0.798	1.556
865I	863.3	43.5	0.829	0.976
865Q	863.7	45.6	0.810	0.976
865U	864.1	48.5	0.753	0.975
935I	931.3	53.2	0.809	0.823

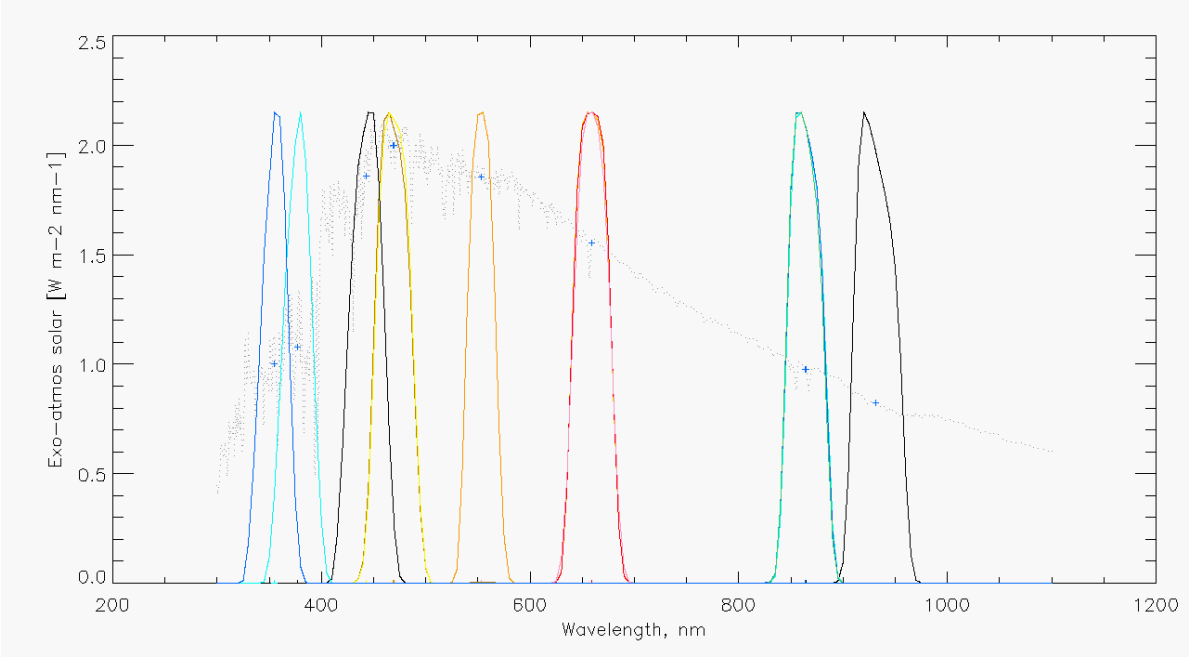

Figure 2. AirMSPI spectral response functions (SRF) shown in colored lines with the Wehrli (1985) exoatmospheric solar irradiance values shown in the faint, gray, dotted line. E0 values at 1 AU are indicated by the "+" symbol.

4 POLARIMETRIC CALIBRATION

GroundMSPI uses a time-varying retardance in the optical path to modulate the orientation of the linearly polarized component of the incoming light, described by the Stokes components Q (excess of horizontally over vertically polarized light) and U (excess of 45º over 135º polarized light) (Diner et al., 2007, 2010; Mahler et al., 2011). As a result, the ratios of these parameters to the radiance I, given by $q = Q/I$ and $u = U/I$ are to first order insensitive to the absolute radiometric calibration of a given pixel because both the numerator and denominator are determined from signals acquired by the same detector element. The degree of linear polarization (DoLP) and angle of linear polarization (AoLP) derived from these ratios, equal to $\sqrt{q^2 + u^2}$ and $0.5\tan^{-1}(u/q)$, respectively, are likewise insensitive to absolute radiometric calibration, based on similar considerations. To compensate for instrumental polarization aberrations (e.g., mirror diattenuation, imperfect retardance), a set of 10 polarimetric calibration coefficients is established for every pixel (Diner et al., 2010).

Results from GroundMSPI (Diner et al., 2012) show systematic DoLP uncertainties (excluding the effects of random noise), determined as the root-mean-square residual in DoLP as a polarizer is rotated in front of the camera, of ±0.003 or better.

5 IMAGE RECTIFICATION AND CO-REGISTRATION

As part of the Level 1B2 data processing, the raw GroundMSPI push-broom imagery is rectified for geometric camera distortions and along-track line-to-line spacing, and the different spectral bands are co-registered onto a common grid. Geometric distortions and band-to-band separations

are captured in the geometric camera model, which is based on Code V ray tracing through the instrument's optical model. The absolute orientation of the focal plane, used to pin-point the camera model, is derived from a geometric calibration experiment in the lab using a collimated light source. Line-to-line spacing in the along-scan direction is directly derived from the input scan rate.

6 INCIDENTAL DATA QUALITY ISSUES

Occasionally, scene elements (e.g., Sun in the image in the principal plane sky measurements) are so bright as to cause saturation in some pixels. Future versions of the GroundMSPI product may flag these situations, but this has not been done for the current version of the publicly available data. Isolated pixels that experienced saturation in one or more channels are readily identifiable in the imagery due to their anomalous appearance. Saturated pixels report a value of -999.0 in the HDF files and appear as black pixels in the JPEG quicklook images. A list of ACEPOL images containing significant saturation, Sun in the image, is provided in Appendix B.

During the data acquisition in Rosamond on 2017-10-25, a film polarizer was taped to the edge of the entrance of GroundMSPI for a few scans for polarimetric validation purposes. The film polarizer is seen by approximately 100 pixels at the edge of the field just prior to the shielded pixels. These pixels will show up as a bright strip in the DoLP image in the JPEG quicklook, because of the high degree of polarization coming out of the polarizer, while the radiance images will show a dark strip, mainly because of the absorption of cross-polarized light. The AoLP image will generally show an angle different than 90° to the scattering plane in the pixels that are covered by the film polarizer, which transmits a fixed polarization angle. A list of ACEPOL images containing the film polarizer is provided in Appendix B.

An artifact of processing is that extra rows are sometimes added to the scan. These datasets have 1000 extra rows at the top of the image and have a value of -999.0 in the HDF files and appear as black pixels in the JPEG quicklook images. A list of the ACEPOL images that have these spurious extra rows is provided in Appendix B.

7 REFERENCES

Diner, D.J., A. Davis, B. Hancock, G. Gutt, R.A. Chipman, and B. Cairns (2007). Dual photoelastic modulator-based polarimetric imaging concept for aerosol remote sensing. *Appl. Opt.* **46**, 8428-8445.

Diner, D.J., A. Davis, B. Hancock, S. Geier, B. Rheingans, V. Jovanovic, M. Bull, D.M. Rider, R.A. Chipman, A. Mahler, and S.C. McClain (2010). First results from a dual photoelastic modulator-based polarimetric camera. *Appl. Opt.* **49**, 2929-2946.

Diner, D.J., F. Xu, J.V. Martonchik, B.E. Rheingans, S. Geier, V.M. Jovanovic, A. Davis, R.A. Chipman, and S.C. and McClain (2012). Exploration of a polarized surface bidirectional reflectance model using the Ground-based Multiangle SpectroPolarimetric Imager. *Atmosphere* **3**, 591-619.

Diner, D.J., F. Xu, M.J. Garay, J.V. Martonchik, B.E. Rheingans, S. Geier, A. Davis, B.R. Hancock, V.M. Jovanovic, M.A. Bull, K. Capraro, R.A. Chipman, and S.C. McClain (2013a). The Airborne Multiangle SpectroPolarimetric Imager (AirMSPI): a new tool for aerosol and cloud remote sensing. *Atmos. Meas. Tech*. **6**, 2007-2025.

Diner, D.J., M.J. Garay, O.V. Kalashnikova, B.E. Rheingans, S. Geier, M.A. Bull, V.M. Jovanovic, F. Xu, C.J. Bruegge, A. Davis, K. Crabtree, and R.A. Chipman (2013b). Airborne Multiangle SpectroPolarmetric Imager (AirMSPI) observations over California during NASA's Polarimeter Definition Experiment (PODEX). *SPIE Proc*. **8873**, 88730B-2.

Jovanovic, V.M., M. Bull, D.J. Diner, S. Geier, and B. Rheingans (2012). Automated data production for a novel Airborne Multiangle SpectroPolarimetric Imager (AirMSPI). *Int. Arch. Photogramm. Remote Sens. Spatial Inf. Sci.*, **XXXIX-B1**, 33-38.

Mahler, A., D.J. Diner, and R.A. Chipman (2011). Analysis of static and time-varying polarization errors in the multiangle spectropolarimetric imager. *Appl. Opt.* **50**, 2080-2087.

Palmer, J.M. (1984). Effective bandwidths for LANDSAT-4 and LANDSAT-D' Multispectral Scanner and Thematic Mapper subsystems. *IEEE Trans. Geosci. Rem. Sens.* **GE-22**, 336-338.

Wehrli, C. (1985). "Extraterrestrial Solar Spectrum", Publication no. 615, Physikalisch Meteorologisches Observatorium + World Radiation Center (PMO/WRC) Davos Dorf, Switzerland, July 1985.

Xu, F., A.B. Davis, R.A. West, and L.W. Esposito (2010). Markov chain formalism for polarized light transfer in plane-parallel atmospheres, with numerical comparison to the Monte Carlo method, *Opt. Express* **19**, 946-967.

8 APPENDIX A: ACRONYM LIST

ACEPOL	Aerosol Characterization from Polarimeter and Lidar
AFRC	Armstrong Flight Research Center
AirHARP	Airborne Hyper-Angular Rainbow Polarimeter
AirMSPI	Airborne Multiangle SpectroPolarimetric Imager
AoLP	Angle of Linear Polarization
ASD	Analytical Spectral Devices
ASDC	Atmospheric Science Data Center
AU	Astronomical Unit
CPL	Cloud Physics Lidar
DEM	Digital Elevation Model
DN	Digital Number
DoLP	Degree of Linear Polarization
EOS	Earth Observing System
GCP	Ground Control Point
GroundMSPI	Ground-Based Multiangle SpectroPolarimetric Imager
HDF-EOS	Hierarchical Data Format for EOS
HSRL-2	High Spectral Resolution Lidar-2
JPL	Jet Propulsion Laboratory
LaRC	Langley Research Center (NASA)
LED	Light Emitting Diode
MISR	Multi-angle Imaging SpectroRadiometer
NaN	Not a Number
NASA	National Aeronautics and Space Administration
NED	National Elevation Dataset
NIST	National Institute of Standards and Technology
PEM	Photoelastic Modulator
RDQI	Radiometric Data Quality Indicator
RSP	Research Scanning Polarimeter
SCF	Science Computing Facility
SDP	Science Data Processing
SI	*Système international*
SPEX	Spectropolarimeter for Planeatary EXploration
SRF	Spectral Response Function
USGS	United States Geological Survey

UTM	Universal Transverse Mercator
UV	Ultraviolet
WGS84	World Geodetic System 1984

9 APPENDIX B

Images containing saturated pixels:

GroundMSPI_L1B2_20171025_170926Z_Rosamond_Principal_Plane_0deg_315U_F01_V009
GroundMSPI_L1B2_20171025_173957Z_Rosamond_Principal_Plane_0deg_323U_F01_V009
GroundMSPI_L1B2_20171025_180951Z_Rosamond_Principal_Plane_0deg_331U_F01_V009
GroundMSPI_L1B2_20171025_183945Z_Rosamond_Principal_Plane_0deg_340U_F01_V009
GroundMSPI_L1B2_20171025_190950Z_Rosamond_Principal_Plane_0deg_349U_F01_V009
GroundMSPI_L1B2_20171025_194011Z_Rosamond_Principal_Plane_0deg_359U_F01_V009
GroundMSPI_L1B2_20171107_194318Z_Fresno_ER2_path_358U_F01_V009
GroundMSPI_L1B2_20171107_183314Z_Fresno_Principal_Plane_0deg_340U_F01_V009
GroundMSPI_L1B2_20171107_184807Z_Fresno_Principal_Plane_0deg_344U_F01_V009
GroundMSPI_L1B2_20171107_190311Z_Fresno_Principal_Plane_0deg_348U_F01_V009
GroundMSPI_L1B2_20171107_191806Z_Fresno_Principal_Plane_0deg_352U_F01_V009
GroundMSPI_L1B2_20171107_193312Z_Fresno_Principal_Plane_0deg_357U_F01_V009
GroundMSPI_L1B2_20171107_194822Z_Fresno_Principal_Plane_0deg_2U_F01_V009
GroundMSPI_L1B2_20171107_200308Z_Fresno_Principal_Plane_0deg_6U_F01_V009
GroundMSPI_L1B2_20171107_201810Z_Fresno_Principal_Plane_0deg_11U_F01_V009
GroundMSPI_L1B2_20171107_203313Z_Fresno_Principal_Plane_0deg_15U_F01_V009
GroundMSPI_L1B2_20171107_204811Z_Fresno_Principal_Plane_0deg_19U_F01_V009
GroundMSPI_L1B2_20171107_210304Z_Fresno_Principal_Plane_0deg_23U_F01_V009
GroundMSPI_L1B2_20171107_211808Z_Fresno_Principal_Plane_0deg_27U_F01_V009
GroundMSPI_L1B2_20171107_213316Z_Fresno_Principal_Plane_0deg_31U_F01_V009
GroundMSPI_L1B2_20171107_214805Z_Fresno_Principal_Plane_0deg_35U_F01_V009

Images containing a film polarizer:

GroundMSPI_L1B2_20171025_170926Z_Rosamond_Principal_Plane_0deg_315U_F01_V009
GroundMSPI_L1B2_20171025_171427Z_Rosamond_Principal_Plane_90deg_45U_F01_V009
GroundMSPI_L1B2_20171025_170228Z_Rosamond_Principal_Plane_0deg_317D_F01_V009
GroundMSPI_L1B2_20171025_170539Z_Rosamond_South_3D_F01_V009

Images containing extra rows:

GroundMSPI_L1B2_20171025_190247Z_Rosamond_Principal_Plane_0deg_351D_F01_V009
GroundMSPI_L1B2_20171025_193253Z_Rosamond_Principal_Plane_0deg_1D_F01_V009